Sébastien Briot
Institut de Recherche en Communications
et Cybernétique de Nantes (IRCCyN),
UMR CNRS 6597,
Nantes 44321, France
e-mail: Sebastien.Briot@irccyn.ec-nantes.fr

Sébastien Krut
Laboratoire d'Informatique,
de Robotique et de Microélectronique
de Montpellier (LIRMM),
UMR CNRS 5506,
Montpellier 34095, France
e-mail: sebastien.krut@lirmm.fr

Maxime Gautier
Institut de Recherche en Communications
et Cybernétique de Nantes (IRCCyN),
Université de Nantes, UMR CNRS 6597,
Nantes 44321, France
e-mail: Maxime.Gautier@irccyn.ec-nantes.fr

Dynamic Parameter Identification of Overactuated Parallel Robots

Offline robot dynamic identification methods are based on the use of the inverse dynamic identification model (IDIM), which calculates the joint forces/torques (estimated as the product of the known control signal (the input reference of the motor current loop) with the joint drive gains) that are linear in relation to the dynamic parameters, and on the use of the linear least squares technique to calculate the parameters (IDIM-LS technique). However, as actuation-redundant parallel robots are overactuated, their IDIM has an infinity of solution for the force/torque prediction, depending on the value of the desired overconstraint that is a priori unknown in the identification process. As a result, the IDIM cannot be used as it is for such a class of parallel robots. This paper proposes a procedure for the dynamic parameter identification of actuation-redundant parallel robots. The procedure takes advantage of two possible modified formulations for the IDIM of actuation-redundant robots that can be used for identification purpose. The modified IDIM formulations project some or all input torques/forces onto the robot bodies, thus leading to a unique solution of the model that can then be used in the identification process. A systematic and straightforward way to compute these modified IDIM is presented. The identification of the inertial parameters of a planar parallel robot with actuation redundancy, the DualV, is then carried out using these modified IDIM. Experimental results show the validity of the methods. [DOI: 10.1115/1.4030867]

1 Introduction

Parallel robots have increasingly been used for a few decades. This is due to their main advantages over serial counterparts that are: (1) higher intrinsic rigidity, (2) larger payload-to-weight ratio, and (3) higher velocity and acceleration capacities [1]. However, their main drawback is probably the presence of singularities in the workspace. In order to overcome this difficulty, actuation redundancy can be used [2,3]. Actuation redundancy occurs when normally passive joints are replaced by active ones. The robot becomes overconstrained. Overconstraints can be smartly used to improve the robot properties, such as increasing the acceleration or payload capacities [4] or even decreasing the backlash [5]. However, this involves the use of more complicated controllers.

Several control approaches could be envisaged [6,7], but it appears that, for high-speed robots or when varying loads have to be compensated (e.g., in pick-and-place operations or machining), computed torque control gives the best results [5,8]. This approach requires an accurate estimation of the dynamic model of the robot with the load [9]. However, a priori inertial parameters extracted from computer-aided design are generally not given by the manufacturer, and even if they are given: (1) they may be inaccurate and (2) friction terms inside the drive trains and passive joints are still unknown. Therefore, the identification of dynamic parameters is necessary.

Several schemes have been proposed in the literature to identify the dynamic parameters of robots [10–16]. Most of the dynamic offline identification methods use an IDIM that gives linear relations between each joint force/torque and the dynamic parameters, build an overdetermined linear system of equations obtained by sampling the IDIM while the robot is tracking some trajectories in position closed-loop control, and estimate the parameter values using LS techniques.

Good experimental results can be obtained if two main conditions are satisfied: joint velocities and accelerations are calculated by a well-tuned derivative bandpass filtering of joint position, and accurate values for joint drive gains are known to calculate the joint force/torque as the products of input references of the motor current loop and joint drive gains [17–19].

For identifying the dynamic parameters of actuation-redundant parallel robots, a major problem arises. To better understand it, let us consider the simple example shown in Fig. 1. This mechanism with one degree-of-freedom (DOF) is moved through the use of two actuators mounted in parallel that can apply two independent forces denoted as f_1 and f_2 on the moving body of mass m. In this example, only the moving mass m is considered (the robot legs are massless). For moving the mechanism, an infinity of possible forces exists, e.g., $[f_1\ f_2] = [m\ddot{x}\ 0]$, or also $[f_1\ f_2] = [0\ m\ddot{x}]$, and even $[f_1\ f_2] = 0.5[m\ddot{x}\ m\ddot{x}]$ or many other force combinations $[f_1\ f_2] = m[(1-\alpha)\ddot{x}\ \alpha\ddot{x}]$ for any value of α. This is due to the fact that, for an overactuated mechanism, the input efforts are not independent (indeed for this mechanism, we have $f_1 = m\ddot{x} - f_2$), which leads to the fact that the generalized efforts are not the mechanism input efforts, but a linear combination of them.

It should be mentioned here that the function $c = |f_1 - f_2|$ is called the overconstraint. As a result, the mechanism IDIM would

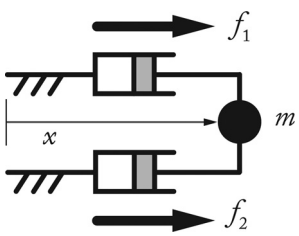

Fig. 1 A 1DOF robot with actuation redundancy

Contributed by the Dynamic Systems Division of ASME for publication in the Journal of Dynamic Systems, Measurement, and Control. Manuscript received June 2, 2014; final manuscript received June 12, 2015; published online August 3, 2015. Assoc. Editor: Srinivasa M. Salapaka.

take the form $[f_1\ f_2] = \mathbf{IDM}_\alpha m$, where $\mathbf{IDM}_\alpha = [(1-\alpha)\ddot{x}\ \alpha\ddot{x}]$ is the observation matrix. $\mathbf{IDM}_\alpha$ depends on the parameter α which is *a priori* unknown. This issue prevents the use of the usual IDIM in the identification process as a unique formulation cannot be defined.[1] This problem also appears for any kind of actuation-redundant parallel robots: their inverse dynamic model is not unique and depends of the overconstraint in the mechanism [5].

It should be mentioned that the overconstraint could be fixed using a proper controller [20]. However, as shown by our own experience in the field, most of the time, manufacturers of industrial robots do not want to provide information on their controller, or even, in worst cases, the controller does not fix the overcontraint. In such cases, the value of the overconstraint cannot be considered as a priori known in the identification process as this quantity cannot be measured. Thus, identification using the usual IDIM for redundant parallel robots cannot be carried out.

To avoid the potential lack of information from the controller, another method should be proposed. Considering again the simple system presented in Fig. 1, it can be demonstrated that its dynamics can be uniquely described if the equations are projected not on the actuators as usual, but on the moving body such that: $f_1 + f_2 = m\ddot{x}$. Thus, by projecting the dynamic equations on a body different from the actuators, a modified IDIM formulation can be obtained. Contrary to the usual IDIM, this modified formulation does not express anymore the linear relations between *each* joint force and the dynamic parameters, but between *a linear combination of the joint forces* and the dynamic parameters. It should be mentioned that this formulation can be used in any case, the value of the overconstraint $c = |f_1 - f_2|$ being known or not.

The aim of this paper is to generalize the approach to any kind of actuation-redundant parallel robots and to propose a systematic and straightforward procedure for their dynamic parameter identification. This procedure is based on the computation of a modified IDIM, linear with respect to the inertial parameters, that does not require the knowledge of the overconstraint. Two different ways for computing the IDIM are proposed. These formulations also minimize the number of intermediate variables and operators used for the symbolic computation of the model. This point is crucial in identification as it minimizes the risk of error propagation (due to the measurement noise) in the computation of the observation matrix.

This systematic procedure is applied for the identification of a 3DOF planar parallel robot with actuation redundancy designed at the LIRMM and named the DualV [21].

A first condensed version of this paper has been proposed in Ref. [22]. Differences with the present paper are: a modified formulation is given for the computation of the IDIM of general parallel robots, in order to better explain the physical meaning of the equations. Another new way to obtain an IDIM is shown and parameters estimated using this IDIM are compared with those obtained using the method developed in Ref. [22]. New experiments and cross-validations have been performed and are presented in this paper.

2 IDIM of Parallel Robots With No Actuation Redundancy

This section presents some recalls on the computation of the IDIM of parallel robots without actuation redundancy. These recalls are necessary as the computation of the IDIM of actuation-redundant parallel robots is partially based on some mathematical derivations shown in this part and to understand why the usual IDIM cannot be used in the identification procedure.

[1]It should be mentioned that in such a simple case, the value of the parameter α could be identified at each time interval, but this cannot be the case for a more general overactuated parallel robot.

2.1 Computation of the IDIM for Parallel Robots With No Actuation Redundancy.

A parallel robot is a complex multibody system having several closed-loops (Fig. 2(*a*)). It is composed of a moving platform connected to a fixed base by n legs, each composed of m_i elements. It is considered here that there is one actuator per leg, but the method can be easily extended to robots with several actuators for each leg.

The computation of IDIM of parallel robots with *no actuation redundancy* is decomposed into two steps [23]:

(1) All closed-loops are virtually opened to virtually disassemble the platform from the rest of the structure (Fig. 2(*b*)); each leg joint is virtually considered to be actuated (even for unactuated actual joints) so that the robot becomes a virtual tree structure while the moving platform becomes a virtual free body; the dynamic models of the virtual tree structure and of the virtual free platform are then computed with a systematic procedure based on the Newton–Euler principle and
(2) the loops are then closed using loop-closure equations and Lagrange multipliers (which represent the joint constraints applied to the platform that are required to close the loops of the real robot), which involve the computation of robot Jacobian matrices.

In what follows, the computation of the IDIM of the virtual tree structure and of the platform is recalled, and then a straightforward way to compute the Jacobian matrices required to calculate the closed-loop constraints is detailed.

2.2 IDIM of Tree Open-Loop Robots.

According to Ref. [14], the complete rigid dynamic model of any open-loop tree structure can be linearly written in terms of a $(n_t \times 1)$ vector with respect to the standard dynamic parameters χ_{st_t} (n_t denotes the total number of joints for the virtual tree structure)

$$\tau_{idm_t}(\mathbf{q}_t, \dot{\mathbf{q}}_t, \ddot{\mathbf{q}}_t) = \mathbf{IDM}_{st_t}(\mathbf{q}_t, \dot{\mathbf{q}}_t, \ddot{\mathbf{q}}_t)\chi_{st_t} \tag{1}$$

where τ_{idm_t} is the $(n_t \times 1)$ vector of the input efforts of the virtual tree structure, $\mathbf{IDM}_{st_t}$ is the $(n_t \times n_{st_t})$ Jacobian matrix of τ_{idm_t} with respect to the $(n_{st_t} \times 1)$ vector χ_{st_t} of the standard dynamic parameters given by $\chi_{st_t}^T = [\chi_{st}^{11T}, \chi_{st}^{21T}, \ldots \chi_{st}^{m_n,nT}]$, and $\mathbf{q}_t, \dot{\mathbf{q}}_t, \ddot{\mathbf{q}}_t$ are the vectors of all joint positions, velocities, and accelerations of the virtual tree structure robot, respectively.

For rigid robots, the vector χ_{st}^{jk} of link j for leg k (denoted in what follows as the link jk) is composed of 14 standard dynamic parameters, such that

$$\chi_{st}^{jk} = \left[xx_{jk}\ xy_{jk}\ xz_{jk}\ yy_{jk}\ yz_{jk}\ zz_{jk}\ mx_{jk}\ my_{jk}\ mz_{jk}\ m_{jk}\ ia_{jk}\ fv_{jk}\ fs_{jk}\ \tau_{off_{jk}}\right]^T \tag{2}$$

where xx_{jk}, xy_{jk}, xz_{jk}, yy_{jk}, yz_{jk}, and zz_{jk} are the six independent components of the inertia matrix $\mathbf{I}_{jk}$ of link jk at the origin of frame jk, i.e.,

$$\mathbf{I}_{jk} = \begin{bmatrix} xx_{jk} & xy_{jk} & xz_{jk} \\ xy_{jk} & yy_{jk} & yz_{jk} \\ xz_{jk} & yz_{jk} & zz_{jk} \end{bmatrix} \tag{3}$$

m_{jk} is its mass and mx_{jk}, my_{jk}, and mz_{jk} are the three components of the first moment of link jk, i.e.,

$$m_{jk}^{jk}\overrightarrow{\mathbf{O}_{jk}\mathbf{S}_{jk}} = [\,mx_{jk} \quad my_{jk} \quad mz_{jk}\,]^T \tag{4}$$

where ${}^{jk}\overrightarrow{\mathbf{O}_{jk}\mathbf{S}_{jk}}$ is the position of the center of mass of the link jk expressed in the frame attached at the origin of the considered link [14], ia_{jk} is the total inertia moment for rotor and gears of the

drive train, fv_{jk} and fs_{jk} are the viscous and Coulomb friction coefficients in the joint jk, respectively, and $\tau_{\text{off}_{jk}} = \tau_{\text{off}fs_{jk}} + \tau_{\text{off}\tau_{jk}}$ is an offset parameter which regroups the current amplifier offset $\tau_{\text{off}\tau_{jk}}$ and the asymmetrical Coulomb friction coefficient $\tau_{\text{off}fs_{jk}}$ such as the friction effort $\tau_{f_{jk}}$ in the joint jk is given by the relation

$$\tau_{f_{jk}} = fv_{jk}\ \dot{q}_{jk} + fs_{jk}\ \text{sign}(\dot{q}_{jk}) + \tau_{\text{off}_{jk}} \tag{5}$$

where $\dot{q}_{jk}$ is the joint jk generalized velocity.

In the same way, the IDIM of the platform can be obtained as

$$\tau_p(\mathbf{x}, \mathbf{t}, \dot{\mathbf{t}}) = \mathbf{IDM}_p(\mathbf{x}, \mathbf{t}, \dot{\mathbf{t}})\chi_p \tag{6}$$

where τ_p is the (6×1) vector of platform reaction wrench, $\mathbf{IDM}_p$ is the (6×10) Jacobian matrix of τ_p, with respect to the (10×1) vector χ_p of the platform inertial standard parameters,[2] and $\mathbf{x}, \mathbf{t}, \dot{\mathbf{t}}$ are the platform pose, twist, and acceleration quantities, respectively.

Various methods can be used to systematically derive these equations. Here, an algorithm based on the use of the modified Denavit–Hartenberg robot geometric description and the Newton–Euler principle is applied. This modeling is known to give the dynamic model equations in the most compact form [14].

2.3 IDIM of Parallel Robots With No Actuation Redundancy. The IDIM of the virtual tree structure and of the free moving platform does not take into account the closed-loop characteristics of parallel robots: among all joint and platform coordinates $\mathbf{q}_t$ and $\mathbf{x}$ of the virtual robot (Fig. 2(*b*)), only a subset denoted as $\mathbf{q}$ is independent in the real robot (actual actuated joints positions are indeed a subset of $\mathbf{q}_t$). All these variables are linked through the loop-closure equations of the real robot that can be obtained by expressing the (translational and rotational) displacement $\mathbf{x}_k$ of the last joints of each leg located at $C_{m_k,k}$ (that belong to both platform and leg k—Fig. 2) in two different ways: (1) as a function of the platform coordinates $\mathbf{x}$ and (2) as a function of all joint coordinates $\mathbf{q}_t$ (also corresponding to the joint coordinates of the virtual tree structure), such that

$$\mathbf{f}(\mathbf{x}, \mathbf{q}_t) = \begin{bmatrix} \mathbf{x}_1(\mathbf{x}) - \mathbf{x}_1(\mathbf{q}_t) \\ \vdots \\ \mathbf{x}_n(\mathbf{x}) - \mathbf{x}_n(\mathbf{q}_t) \end{bmatrix} = \mathbf{0} \tag{7}$$

The main problem with Eq. (7) is that it is usually difficult to straightforwardly solve these equations. Therefore, it is better to express the reduced loop-closure equations of the parallel robot, which are known to be simpler to obtain [1] and that directly relate the displacements $\mathbf{q}$ of the actuated joints to the moving platform independent coordinates $\mathbf{x}_{\text{ind}}$ (defined as a subset of $\mathbf{x}$)

$$\mathbf{f}_p(\mathbf{x}_{\text{ind}}, \mathbf{q}) = \mathbf{0} \tag{8}$$

and to solve then the reduced forward kinematic problem (FKP) gives $\mathbf{x}_{\text{ind}}$ as a function of $\mathbf{q}$. Obviously, this problem can be also tedious, but Eq. (8) is simpler to solve than Eq. (7), if the problem cannot be solved analytically, a numeric procedure may be applied [1].

Once the values of $\mathbf{x}_{\text{ind}}$ are found as a function of $\mathbf{q}$, it is possible to solve the inverse kinematic problem using Eq. (7) in order to express all joint coordinates as a function of $\mathbf{x}$ (that is function of $\mathbf{x}_{\text{ind}}$), and thus of $\mathbf{q}$. This problem is generally easy for usual parallel robots [1] and, even for more complicated cases, can now be solved using advanced mathematical methods [24].

Differentiating Eqs. (7) and (8) with respect to time, the following expressions can be obtained:

$$\mathbf{J}_{tk}\mathbf{v} - \mathbf{J}_k\dot{\mathbf{q}}_t = \mathbf{0} \Rightarrow \dot{\mathbf{q}}_t = \mathbf{J}_k^{-1}\mathbf{J}_{tk}\mathbf{v} \tag{9}$$

$$\begin{aligned} &\mathbf{J}_{tk}\dot{\mathbf{v}} + \dot{\mathbf{J}}_{tk}\mathbf{v} - \mathbf{J}_k\ddot{\mathbf{q}}_t - \dot{\mathbf{J}}_k\dot{\mathbf{q}}_t = \mathbf{0} \\ &\Rightarrow \ddot{\mathbf{q}}_t = \mathbf{J}_k^{-1}(\mathbf{J}_{tk}\dot{\mathbf{v}} + \dot{\mathbf{J}}_{tk}\mathbf{v} - \dot{\mathbf{J}}_k\dot{\mathbf{q}}_t) \end{aligned} \tag{10}$$

and

$$\mathbf{A}_p\mathbf{v} + \mathbf{B}_p\dot{\mathbf{q}} = \mathbf{0} \Rightarrow \mathbf{v} = -\mathbf{A}_p^{-1}\mathbf{B}_p\dot{\mathbf{q}} = \mathbf{J}_p\dot{\mathbf{q}}, \tag{11}$$

$$\begin{aligned} &\mathbf{A}_p\dot{\mathbf{v}} + \dot{\mathbf{A}}_p\mathbf{v} + \mathbf{B}_p\ddot{\mathbf{q}} + \dot{\mathbf{B}}_p\dot{\mathbf{q}} = \mathbf{0} \\ &\Rightarrow \dot{\mathbf{v}} = -\mathbf{A}_p^{-1}(\dot{\mathbf{A}}_p\mathbf{v} + \mathbf{B}_p\ddot{\mathbf{q}} + \dot{\mathbf{B}}_p\dot{\mathbf{q}}) \end{aligned} \tag{12}$$

where

$$\begin{aligned} \mathbf{A}_p &= \left[\frac{\partial \mathbf{f}_p}{\partial \mathbf{x}_{\text{ind}}}\right]\mathbf{T}, \quad \mathbf{B}_p = \left[\frac{\partial \mathbf{f}_p}{\partial \mathbf{q}}\right] \\ \mathbf{J}_{tk} &= \left[\frac{\partial \mathbf{f}'}{\partial \mathbf{x}_{\text{ind}}}\right], \quad \mathbf{J}_k = -\left[\frac{\partial \mathbf{f}'}{\partial \mathbf{q}_t}\right] \end{aligned} \tag{13}$$

with $\mathbf{f}'$ a subset of n_t independent equations in $\mathbf{f}$ ($n_t = \sum_{i=1}^{n} m_i$), $\mathbf{T}$ a transformation matrix between the platform twist $\mathbf{t}$ and the derivatives with respect to time of the terms $\mathbf{x}_{\text{ind}}$ [1], and $\mathbf{v}$ a vector of the independent coordinates in the platform twist $\mathbf{t}$ ($\dim \mathbf{v} = \dim \mathbf{x}_{\text{ind}} = n \leq 6$), defined such that

$$\mathbf{t} = \mathbf{D}\mathbf{v} \tag{14}$$

In the case of robots with 6DOF, $\mathbf{D}$ is the identity matrix. In these expressions, it should be noted that the matrix $\mathbf{J}_k$ stacks all Jacobian matrices corresponding to the independent motions of the last joint due to the joint displacements of each serial leg and is thus a square matrix of dimension $(n_t \times n_t)$, the matrix $\mathbf{J}_{tk}$ is a matrix of dimension $(n_t \times n)$ that can be obtained by considering the rigid body displacement of any point of the robot platform as a function of the platform twist, and in the case of parallel robots without actuation redundancy, the matrices $\mathbf{A}_p$ and $\mathbf{B}_p$ are square of dimension $(n \times n)$.

Finally, by introducing Eqs. (11) and (12) into Eqs. (9) and (10), the expressions of $\dot{\mathbf{q}}_t$ and $\ddot{\mathbf{q}}_t$ as functions of $\mathbf{q}$, $\dot{\mathbf{q}}$, and $\ddot{\mathbf{q}}$ can be obtained. It should be mentioned that all the previous expressions are valuable as long as the robot does not meet any singularity and as long as there is the same number of actuators as the number of platform DOF to control. The singularity avoidance or crossing is not the main topic of this paper, and the reader should refer to Refs. [25] and [26] for further developments. In the following of Sec. 2.3, it is considered that all these matrices are regular.

To take into account the loop-closure constraints into the dynamic model of the parallel robot, Lagrange multipliers $\lambda^{\text{T}} = \begin{bmatrix}\lambda_1^{\text{T}} & \lambda_2^{\text{T}}\end{bmatrix}$ can be used [14] to compute the $(n \times 1)$ vector of the actuated joint force/torque τ_{idm} of the closed-loop structure. τ_{idm} can be obtained in relation of the Lagrange multipliers λ by

$$\tau_{\text{idm}} = [\mathbf{0}, -\mathbf{B}_p^{\text{T}}]\begin{bmatrix}\lambda_1 \\ \lambda_2\end{bmatrix} = -\mathbf{B}^{\text{T}}\lambda \tag{15}$$

where λ is calculated from the relation

$$\begin{bmatrix}\mathbf{J}_k^{\text{T}} & \mathbf{0} \\ -\mathbf{J}_{tk}^{\text{T}} & \mathbf{A}_p^{\text{T}}\end{bmatrix}\begin{bmatrix}\lambda_1 \\ \lambda_2\end{bmatrix} = \mathbf{A}^{\text{T}}\lambda = \begin{bmatrix}\tau_{\text{idm}_t} \\ \tau_{\text{pr}}\end{bmatrix} \tag{16}$$

In these expressions, λ_1 stacks the wrenches λ_1^1 to λ_1^n (Fig. 2(*b*)) applied by the virtual tree structure on the platform at points

[2]The number of standard parameters of a free rigid body can be reduced to ten inertial parameters as it is not necessary to consider the parameters ia_j, fv_j, fs_j, and τ_{off_j} related to actuated joint drive chains.

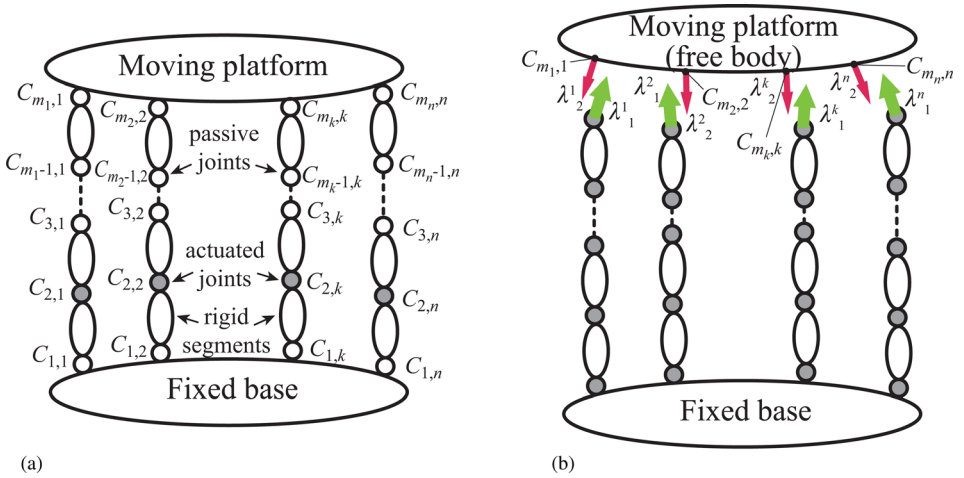

Fig. 2 A general parallel robot (gray circles denote actuated joints): (*a*) Kinematic chain ($C_{i,j}$ is the joint j of the leg k, and m_k is the total number of joints for the leg k) and (*b*) virtual tree structure

$C_{m_k,k}$, so that that virtual structure can have the same motion as the real parallel robot, λ_2 stacks the values of the norms of the wrenches λ_2^1 to λ_2^n (Fig. 2(*b*)) due to the platform dynamics in the platform joints located at $C_{m_k,k}$, $\mathbf{A}$ is a square matrix of dimension $((n_t+n)\times(n_t+n))$, and τ_{pr} is defined by

$$\tau_{pr} = \mathbf{D}^T \tau_p \tag{17}$$

where τ_p is given in Eq. (6), and τ_{pr} is a subset of forces/moments in τ_p that can be found through the use of the principle of virtual powers, which states that

$$\mathbf{v}^{*T}\tau_{pr} = \mathbf{t}^{*T}\tau_p = \mathbf{v}^{*T}\mathbf{D}^T\tau_p \tag{18}$$

In this equation, the superscript " * " stands for a virtual velocity.

Thus, the second equation of the system (16) represents the platform equilibrium so that the loops of the parallel robot can be closed.

Solving Eqs. (15) and (16), it can be demonstrated that

$$\begin{aligned}\tau_{idm} &= \mathbf{J}_t^T\tau_{idm_t} + \mathbf{J}_p^T\mathbf{D}^T\tau_p \\ &= \mathbf{J}_t^T\mathbf{IDM}_{st_t}\chi_{st_t} + \mathbf{J}_p^T\mathbf{D}^T\mathbf{IDM}_p\chi_p \\ &= \begin{bmatrix}\mathbf{J}_t^T\mathbf{IDM}_{st_t} & \mathbf{J}_p^T\mathbf{D}^T\mathbf{IDM}_p\end{bmatrix}\begin{bmatrix}\chi_{st_t}^T & \chi_p^T\end{bmatrix}^T \\ &= \mathbf{IDM}_{st}(\mathbf{q},\dot{\mathbf{q}},\ddot{\mathbf{q}})\chi_{st}\end{aligned} \tag{19}$$

where $\mathbf{J}_t = \mathbf{J}_k^{-1}\mathbf{J}_{tk}\mathbf{J}_p$.

Equation (19) represents the IDIM of the parallel robot without actuation redundancy.

3 IDIM of Parallel Robots With Actuation Redundancy

3.1 Inverse Dynamic Model. Let us consider in this part an actuation-redundant parallel robot with r independent DOF controlled by n actuators, where $r<n$. Differentiating Eq. (7) with respect to time, it can now be proven that the matrix $\mathbf{A}_p$ of Eq. (11) becomes rectangular of dimension $(n\times r)$, while the matrix $\mathbf{B}_p$ stays square of dimension $(n\times n)$ [1].

As a result, the right parts of Eqs. (11) and (12) must be changed as

$$\mathbf{A}_p\mathbf{v} + \mathbf{B}_p\dot{\mathbf{q}} = \mathbf{0} \Rightarrow \dot{\mathbf{q}} = -\mathbf{B}_p^{-1}\mathbf{A}_p\mathbf{v} = \mathbf{J}_p^{inv}\mathbf{v} \tag{20}$$

or

$$\mathbf{v} = \mathbf{J}_p^{inv+}\dot{\mathbf{q}} \tag{21}$$

where $\mathbf{J}_p^{inv+}$ is the pseudo-inverse of $\mathbf{J}_p^{inv}$ defined by

$$\mathbf{J}_p^{inv+} = \left(\mathbf{J}_p^{inv\ T}\mathbf{J}_p^{inv}\right)^{-1}\mathbf{J}_p^{inv\ T} \tag{22}$$

and

$$\begin{aligned}&\mathbf{A}_p\dot{\mathbf{v}} + \dot{\mathbf{A}}_p\mathbf{v} + \mathbf{B}_p\ddot{\mathbf{q}} + \dot{\mathbf{B}}_p\dot{\mathbf{q}} = \mathbf{0} \\ &\Rightarrow \ddot{\mathbf{q}} = -\mathbf{B}_p^{-1}(\dot{\mathbf{A}}_p\mathbf{v} + \mathbf{A}_p\dot{\mathbf{v}} + \dot{\mathbf{B}}_p\dot{\mathbf{q}})\end{aligned} \tag{23}$$

or also

$$\dot{\mathbf{v}} = -\mathbf{A}_p^{+}(\dot{\mathbf{A}}_p\mathbf{v} + \mathbf{B}_p\ddot{\mathbf{q}} + \dot{\mathbf{B}}_p\dot{\mathbf{q}}) \tag{24}$$

where $\mathbf{A}_p^+$ is the pseudo-inverse of $\mathbf{A}_p$ defined by

$$\mathbf{A}_p^{+} = \left(\mathbf{A}_p^T\mathbf{A}_p\right)^{-1}\mathbf{A}_p^T \tag{25}$$

Moreover, the matrix $\mathbf{A}^T$ of Eq. (16) becomes now a rectangular matrix with (n_t+r) rows and (n_t+n) columns, i.e., the system (16) has more unknowns than equations. Thus, there is an infinity of solution for the Lagrange multipliers λ. One solution can be obtained, assuming that the value of the overconstraint $\mathbf{c}$ in the robot is known [5]

$$\begin{aligned}\tau_{idm} &= [\mathbf{0}, -\mathbf{B}_p^T]\lambda, \\ \lambda &= \left(\mathbf{A}^T\right)^{+}\begin{bmatrix}\tau_{idm_t} \\ \tau_{pr}\end{bmatrix} + \left(\mathbf{I} - \left(\mathbf{A}^T\right)^{+}\mathbf{A}^T\right)\mathbf{c}\end{aligned} \tag{26}$$

where $\left(\mathbf{A}^T\right)^+$ is the Moore–Penrose pseudo-inverse of $\mathbf{A}^T$

$$\left(\mathbf{A}^T\right)^{+} = \mathbf{A}\left(\mathbf{A}^T\mathbf{A}\right)^{-1} \tag{27}$$

that may be obtained through singular value decomposition (SVD). It should be mentioned that, in most of the cases, the value of $\mathbf{c}$ is set to zero in the controller and, as a result, the vector λ is of minimal norm. Obviously, this is not always the case and another (constant or varying) value can be given in order to improve the robot properties, such as increasing the acceleration or payload capacities [4] or even decreasing the backlash [5].

However, as the value of the overcontraint $\mathbf{c}$ is generally not given by industrial controllers, it cannot be set a priori. Thus, the dynamic model (26) cannot be used as it is. We propose here two ways for modifying the inverse dynamic model so that it is possible to obtain a unique IDIM for parallel robot with actuation redundancy. It should be mentioned that these formulations are universal (i.e., they can be obtained for any actuation-redundant parallel robot *for which the value of the overconstraint is known or not*).

3.1.1 Case 1: Projection of the Input Force/Torque on the Platform. As matrices $\mathbf{B}_p$ and $\mathbf{J}_k$ of Eqs. (11) and (9) are still square and not singular outside of serial singularities [1], Eqs. (15) and (16) can be rewritten as

$$\begin{bmatrix} \tau_{\text{idm}} \\ \tau_{\text{idm}_t} \end{bmatrix} = \begin{bmatrix} \mathbf{0} & -\mathbf{B}_p^{\text{T}} \\ \mathbf{J}_k^{\text{T}} & \mathbf{0} \end{bmatrix} \lambda, \quad \begin{bmatrix} -\mathbf{J}_{tk}^{\text{T}} & \mathbf{A}_p^{\text{T}} \end{bmatrix} \lambda = \tau_{\text{pr}} \tag{28}$$

resulting in

$$\begin{aligned} \tau_{\text{pr}} &= \begin{bmatrix} -\mathbf{J}_{tk}^{\text{T}} & \mathbf{A}_p^{\text{T}} \end{bmatrix} \begin{bmatrix} \mathbf{0} & \mathbf{J}_k^{-\text{T}} \\ -\mathbf{B}_p^{-\text{T}} & \mathbf{0} \end{bmatrix} \begin{bmatrix} \tau_{\text{idm}} \\ \tau_{\text{idm}_t} \end{bmatrix} \\ &= \begin{bmatrix} -\mathbf{A}_p^{\text{T}}\mathbf{B}_p^{-\text{T}} & -\mathbf{J}_{tk}^{\text{T}}\mathbf{J}_k^{-\text{T}} \end{bmatrix} \begin{bmatrix} \tau_{\text{idm}} \\ \tau_{\text{idm}_t} \end{bmatrix} \\ &= \begin{bmatrix} \mathbf{J}_p^{\text{inv T}} & -\mathbf{J}_{tk}^{\text{T}}\mathbf{J}_k^{-\text{T}} \end{bmatrix} \begin{bmatrix} \tau_{\text{idm}} \\ \tau_{\text{idm}_t} \end{bmatrix} \end{aligned} \tag{29}$$

with $\mathbf{J}_p^{\text{inv}} = -\mathbf{B}_p^{-1}\mathbf{A}_p$ according to Eq. (20).

Introducing Eqs. (1), (6), and (17) into Eq. (29) leads to

$$\begin{aligned} \Gamma_{\text{idm}}^1 : &= \mathbf{J}_p^{\text{inv T}}\tau_{\text{idm}} = \mathbf{J}_{\text{tk}}^{\text{T}}\mathbf{J}_k^{-\text{T}}\tau_{\text{idm}_t} + \mathbf{D}^{\text{T}}\tau_p \\ &= \mathbf{J}_{\text{tk}}^{\text{T}}\mathbf{J}_k^{-\text{T}}\mathbf{IDM}_{\text{st}_t}\chi_{\text{st}_t} + \mathbf{D}^{\text{T}}\mathbf{IDM}_p\chi_p \\ &= \begin{bmatrix} \mathbf{J}_{\text{tk}}^{\text{T}}\mathbf{J}_k^{-\text{T}}\mathbf{IDM}_{\text{st}_t} & \mathbf{D}^{T}\mathbf{IDM}_p \end{bmatrix} \begin{bmatrix} \chi_{\text{st}_t}^{\text{T}} & \chi_p^{\text{T}} \end{bmatrix}^{\text{T}} \\ &= \mathbf{IDM}_{\text{st}_1}^{\text{red}}(\mathbf{q}, \dot{\mathbf{q}}, \ddot{\mathbf{q}})\chi_{\text{st}} \end{aligned} \tag{30}$$

Thus, by projecting the input forces/torques on the platform through the use of the matrix $\mathbf{J}_p^{\text{inv T}}$, the inverse dynamic model becomes unique and can be used for identification purpose.

3.1.2 Case 2: Projection of Some Input Force/Torque on Actuated Bodies. Another way to compute a unique solution for the inverse dynamic model is the following. The idea is to fulfill the system of equations (16) with $n-r$ equations coming from Eq. (15). Let us partition Eq. (15) as follows:

$$\begin{bmatrix} \tau_{\text{idm}}^{\text{l:}r} \\ \tau_{\text{idm}}^{r+1:n} \end{bmatrix} = \begin{bmatrix} \mathbf{0} & -\mathbf{B}_p^{\text{l:}r}T \\ \mathbf{0} & -\mathbf{B}_p^{r+1:n}T \end{bmatrix} \lambda \tag{31}$$

where $\tau_{\text{idm}}^{\text{l:}r}$ and $\tau_{\text{idm}}^{r+1:n}$ are subsets of τ_{idm} ($\tau_{\text{idm}}^{\text{l:}r}$ is of length r, and $\tau_{\text{idm}}^{r+1:n}$ is of length $n-r$), and $\mathbf{B}_p^{\text{l:}r}$ and $\mathbf{B}_p^{r+1:n}$ are subsets of $\mathbf{B}_p$ ($\mathbf{B}_p^{\text{l:}r}$ is of dimension $r \times n$, and $\mathbf{B}_p^{r+1:n}$ of dimension $(n-r) \times n$).

The way of partitioning Eq. (15) is obviously not unique. If the robot has got identical legs with symmetrical arrangement (this is the case of the prototype studied in Sec. 5.1), the $n-r$ equations can be those corresponding to the $n-r$ last actuators. If it is not the case, a study must be completed to find the partitioning that leads to the best identification results (in terms of quality of parameter estimation and input/force torque reconstruction). However, this study is not the topic of the present paper.

Finally, the $n-r$ last equations of Eq. (31) can be added into Eq. (16) such that the system (15) and (16) becomes

$$\tau_{idm}^{\text{l:}r} = \begin{bmatrix} \mathbf{0} & -\mathbf{B}_p^{\text{l:}r}T \end{bmatrix} \lambda = \mathbf{B}_p^* T\lambda \tag{32}$$

$$\begin{bmatrix} \tau_{\text{idm}}^{r+1:n} \\ \tau_{\text{idm}_t} \\ \tau_{\text{pr}} \end{bmatrix} = \begin{bmatrix} \mathbf{0} & -\mathbf{B}_p^{\text{l:}r}\text{T} \\ \mathbf{J}_k^{\text{T}} & \mathbf{0} \\ -\mathbf{J}_{\text{tk}}^{\text{T}} & \mathbf{A}_p^{\text{T}} \end{bmatrix} \lambda = \mathbf{A}_p^*\text{T}\lambda \tag{33}$$

Solving Eq. (33), it comes that

$$\lambda = \mathbf{A}_p^*{-}\text{T} \begin{bmatrix} \tau_{\text{idm}}^{r+1:n} \\ \tau_{\text{idm}_t} \\ \tau_{\text{pr}} \end{bmatrix} = \mathbf{A}_{p_1}\tau_{\text{idm}}^{r+1:n} + \mathbf{A}_{p_2}\tau_{\text{idm}_t} + \mathbf{A}_{p_3}\tau_{\text{pr}} \tag{34}$$

where $\mathbf{A}_p^*{-}\text{T} = \begin{bmatrix} \mathbf{A}_{p_1} & \mathbf{A}_{p_2} & \mathbf{A}_{p_3} \end{bmatrix}$. It should be mentioned that a sufficient condition for $\mathbf{A}_p^*\text{T}$ to be invertible is that matrices $\mathbf{J}_k^{\text{T}}, \mathbf{J}_{\text{tk}}^{\text{T}}, \mathbf{B}_p^{\text{l:}r}\text{T}$, and $\mathbf{A}_p^{\text{T}}$ are of full rank, i.e., the robot does not cross any serial or parallel singularities [1].

Introducing Eq. (33) into Eq. (32) leads to

$$\begin{aligned} \tau_{\text{idm}}^{\text{l:}r} &= \mathbf{B}_p^*\text{T}\left(\mathbf{A}_{p_1}\tau_{\text{idm}}^{r+1:n} + \mathbf{A}_{p_2}\tau_{\text{idm}_t} + \mathbf{A}_{p_3}\tau_{\text{pr}}\right) \\ &= \mathbf{B}_p^*\text{T}\mathbf{A}_{p_1}^{\text{inv}}\tau_{\text{idm}}^{r+1:n} + \mathbf{B}_p^*\text{T}\mathbf{A}_{p_2}\tau_{\text{idm}_t} + \mathbf{B}_p^*\text{T}\mathbf{A}_{p_3}\tau_{\text{pr}} \\ &= \mathbf{J}_{\tau_{r+1:n}}^{\text{T}}\tau_{\text{idm}}^{r+1:n} + \mathbf{J}_{\tau_{\text{idm}}}^{\text{T}}\tau_{\text{idm}_t} + \mathbf{J}_{\tau_{\text{pr}}}^{\text{T}}\tau_{\text{pr}} \end{aligned} \tag{35}$$

Introducing Eqs. (1), (6), and (17) into Eq. (35) leads to

$$\begin{aligned} \Gamma_{\text{idm}}^2 &= \mathbf{J}_{\tau_{\text{idm}}}^{\text{T}}\tau_{\text{idm}_t} + \mathbf{J}_{\tau_{\text{pr}}}^{\text{T}}\tau_{\text{pr}} \\ &= \mathbf{J}_{\tau_{\text{idm}}}^{\text{T}}\mathbf{IDM}_{\text{st}_t}\chi_{\text{st}_t} + \mathbf{J}_{\tau_{\text{pr}}}^{\text{T}}\mathbf{D}^{\text{T}}\mathbf{IDM}_p\chi_p \\ &= \begin{bmatrix} \mathbf{J}_{\tau_{\text{idm}}}^{\text{T}}\mathbf{IDM}_{\text{st}_t} & \mathbf{J}_{\tau_{\text{pr}}}^{\text{T}}\mathbf{D}^{\text{T}}\mathbf{IDM}_p \end{bmatrix} \begin{bmatrix} \chi_{\text{st}_t}^{\text{T}} & \chi_p^{\text{T}} \end{bmatrix}^{\text{T}} \\ &= \mathbf{IDM}_{\text{st}_2}^{\text{red}}(\mathbf{q}, \dot{\mathbf{q}}, \ddot{\mathbf{q}})\chi_{\text{st}} \end{aligned} \tag{36}$$

where $\Gamma_{\text{idm}}^2 := \tau_{\text{idm}}^{\text{l:}r} - \mathbf{J}_{\tau_{r+1:n}}^{\text{T}}\tau_{\text{idm}}^{r+1:n}$. Thus, by projecting the input forces/torques of $n-r$ actuators on r other actuators, the inverse dynamic model becomes also unique and can be used for identification purpose.

3.2 Computation of the IDIM Including the Payload. Because of perturbations due to noise measurement and modeling errors, the actual force/torque τ differs from τ_{idm}. This involves that the value of Γ^j calculated using the values of the measured force/torques τ differs from Γ_{idm}^j by an error $\mathbf{e}$, such that

$$\Gamma^j = \Gamma_{\text{idm}}^j + \mathbf{e} = \mathbf{IDM}_{\text{st}_j}^{\text{red}}\chi_{\text{st}} + \mathbf{e} \tag{37}$$

Equation (37) represents the IDIM. The payload is considered as an additional link (denoted as link l) fixed to the robot platform [9]. Model (37) then becomes

$$\begin{aligned} \Gamma^j &= \begin{bmatrix} \mathbf{IDM}_{\text{st}_j}^{\text{red}} & \mathbf{IDM}_l \end{bmatrix} \begin{bmatrix} \chi_{\text{st}} \\ \chi_l \end{bmatrix} + \mathbf{e} \\ &= \mathbf{IDM}_{\text{tot}}\chi_{\text{tot}} + \mathbf{e} \end{aligned} \tag{38}$$

where χ_l is the $(n_l \times 1)$ vector of the inertial parameters of the payload; $\mathbf{IDM}_l$ is the $(n \times n_l)$ Jacobian matrix of Γ_{idm}^j with respect to the vector χ_l.

4 Identification Procedure

4.1 Computation of the Base Parameters. In this section, the offline identification of the dynamic parameters is considered,

given measured or estimated offline data for τ and $(\mathbf{q}, \dot{\mathbf{q}}, \ddot{\mathbf{q}})$, collected while the robot is tracking some planned trajectories. The model (37) is sampled at frequency f_m in order to get an overdetermined linear system of r_{f_m} equations and n_{st} unknowns

$$\mathbf{Y}_{f_m}(\hat{\mathbf{q}}, \tau) = \mathbf{W}^{st}_{f_m}(\hat{\mathbf{q}}, \hat{\dot{\mathbf{q}}}, \hat{\ddot{\mathbf{q}}})\chi_{st} + \rho_{f_m} \tag{39}$$

where $(\hat{\mathbf{q}}, \hat{\dot{\mathbf{q}}}, \hat{\ddot{\mathbf{q}}})$ is an estimation of $(\mathbf{q}, \dot{\mathbf{q}}, \ddot{\mathbf{q}})$, respectively, obtained by sampling and bandpass filtering the measure of $\mathbf{q}$ [27], ρ_{f_m} is the $(r_{f_m} \times 1)$ vector of errors, $\mathbf{Y}_{f_m}$ is the $(r_{f_m} \times 1)$ vector of the inputs Γ^j, sampled at frequency f_m, and $\mathbf{W}^{st}_{f_m}(\hat{\mathbf{q}}, \hat{\dot{\mathbf{q}}}, \hat{\ddot{\mathbf{q}}})$ is the $(r_{f_m} \times n_{st})$ observation matrix.

The forces/torques τ (and thus the values of Γ^j) are perturbed by high-frequency unmodeled friction and flexibility force/torque of the joint drive chain which is rejected by the closed-loop control. These force/torque ripples are eliminated with a parallel decimation procedure that low-pass filters in parallel $\mathbf{Y}_{f_m}$ and each column of $\mathbf{W}^{st}_{f_m}$ (in parallel) and resamples them at a lower rate, keeping one sample over n_d. This parallel decimation can be carried out with the MATLAB *decimate* function, where the low-pass filter cutoff frequency, $\omega_{fp} = 2\pi 0.8 f_m/(2n_d)$, is chosen in order to keep $\mathbf{Y}_{f_m}$ and $\mathbf{W}^{st}_{f_m}$ in the frequency range of the model dynamics. After the data acquisition procedure and the parallel decimation of Eq. (39), we obtain an overdetermined linear system

$$\mathbf{Y}(\tau) = \mathbf{W}^{st}(\hat{\mathbf{q}}, \hat{\dot{\mathbf{q}}}, \hat{\ddot{\mathbf{q}}})\chi_{st} + \rho \tag{40}$$

where ρ is the $(r_c \times 1)$ vector of errors, $\mathbf{Y}$ is the $(r_c \times 1)$ vector of the inputs, and $\mathbf{W}^{st}(\hat{\mathbf{q}}, \hat{\dot{\mathbf{q}}}, \hat{\ddot{\mathbf{q}}})$ is the $(r_c \times n_{st})$ observation matrix.

It should be noted that no error is introduced by the parallel filtering process in the linear relation (40) compared with Eq. (39). In Ref. [27], practical rules for tuning this filter are given.

In $\mathbf{Y}$ and $\mathbf{W}^{st}$, the equations corresponding to the jth line of the vector Γ^j and of the matrix $\mathbf{IDM}^{red}_{st_j}$ are sorted in order to regroup the equations of each line altogether such that: $\mathbf{Y}^T = \left[(\mathbf{Y}^1)^T, \ldots, (\mathbf{Y}^n)^T\right], \mathbf{W}^{st} = \left[(\mathbf{W}^1)^T, \ldots, (\mathbf{W}^n)^T\right]^T$, where $\mathbf{Y}^j$ and $\mathbf{W}^j$ represent the r_c/n equations of the jth line of the vector Γ^j and of the matrix $\mathbf{IDM}^{red}_{st_j}$.

The identifiable parameters are the base parameters which are the minimum number of dynamic parameters from which the dynamic model can be calculated [14]. The minimal dynamic model can be written using the n_b base dynamic parameters χ as follows:

$$\mathbf{Y} = \mathbf{W}(\mathbf{q}, \dot{\mathbf{q}}, \ddot{\mathbf{q}})\chi + \rho \tag{41}$$

where $\mathbf{W}$ is a subset of independent columns in $\mathbf{W}^{st}$ which defines the identifiable parameters. Several methods exist for the computation of these subsets (analytical [14] or numerical [28]). In this work, it is preferred to use a numerical method based on *QR* factorization.

There is infinity of possible subsets of base parameters, as presented in Refs. [28] and [29]. In Ref. [29], the authors test different subsets (obtained via the SVD of the observation matrix [28]) and keep the one which leads to the best conditioning index of the observation matrix. Even if it is computationally efficient, this method has a drawback: for a parallel robot with identical legs, it can lead to a set of base parameters which does not conserve the symmetry properties of the robot legs. Obviously, for avoiding this problem, it can be set a priori that some parameters are equivalent, which involves to sum their corresponding columns in the observation matrix. However, as there can be some small variations in the parameters values due to the manufacturing process, it is worth to avoid this a priori regroupment and check it a posteriori on the identified values.

Here, a method is described that avoids these drawbacks. For presenting it, let us make some brief recalls on the computation of the base parameters via *QR* factorization. The *QR* factorization of the matrix $\mathbf{W}^{st}$ of Eq. (40) takes the form

$$\mathbf{Q}^T\mathbf{W}^{st} = \begin{bmatrix} \mathbf{R} \\ \mathbf{0} \end{bmatrix} \tag{42}$$

where $\mathbf{Q}$ is a $(r \times r)$ orthogonal matrix, and $\mathbf{R}$ is upper triangular. If the absolute value $|R_{kk}|$ of the kth component located on the diagonal of $\mathbf{R}$ is inferior to α (α is the numerical rank—different from zero because of round-off errors—and can be chosen such that $\alpha = \epsilon \max|R_{jj}|$, where ϵ is a small coefficient depending on the level of perturbations in $\mathbf{W}^{st}$ (due to noise measurement and error modeling) and $\max|R_{jj}|$ is the largest diagonal absolute value of $\mathbf{R}$ [28]), the kth column $\mathbf{W}^{st}_k$ of $\mathbf{W}^{st}$ can be deleted. At the end of the procedure, $(n_{st} - n_b)$ columns of $\mathbf{W}^{st}$ have been deleted, which correspond to $(n_{st} - n_b)$ standard parameters removed from vector χ_{st} to keep a set of n_b base parameters χ.

Because the *QR* algorithm starts from the last columns to the first of $\mathbf{W}^{st}$, the $(n_{st} - n_b)$ standard parameters to delete are dependent on the ordering of the columns of that matrix. For serial robots, the matrix $\mathbf{W}^{st}$ is built such that the columns with the smaller indices are those corresponding to the links closest from the base. Thus, using the previous algorithm, the parameters with the smallest influence (those of the wrist) are eliminated from the base parameters.

For parallel robots, to take into account the symmetry in the leg dynamic parameters, it is preferable to order the columns of $\mathbf{W}^{st}$, such that

$$\mathbf{W}^{st}_r = \begin{bmatrix} \mathbf{W}^{st}_p & \mathbf{W}^{st}_{\chi_1,1:n} & \mathbf{W}^{st}_{\chi_2,1:n} & \cdots & \mathbf{W}^{st}_{\chi_{n_{st_{leg}}},1:n} \end{bmatrix} \tag{43}$$

where $n_{st_{leg}}$ is the number of standard parameters for one leg, matrix $\mathbf{W}^{st}_p$ is the observation matrix corresponding to the platform inertial parameters, and matrices $\mathbf{W}^{st}_{\chi_k,1:n}$ concatenate the columns of matrix $\mathbf{W}^{st}$ corresponding to the parameters χ_k that are a priori identical for the n legs. Then, $(n_{st} - n_b)$ columns of $\mathbf{W}^{st}_r$ can be deleted using the previous approach based on the *QR* factorization to obtain a new observation matrix $\mathbf{W}$ associated with a set of symmetrical base parameters denoted as χ.

4.2 Weighted Least Square Identification of the Robot Dynamic Parameters (IDIM-WLS). The LS solution $\hat{\chi}$ of Eq. (41) is given by

$$\hat{\chi} = \mathbf{W}^+\mathbf{Y} \text{ where } \mathbf{W}^+ = (\mathbf{W}^T\mathbf{W})^{-1}\mathbf{W}^T \tag{44}$$

is computed using the *QR* factorization of $\mathbf{W}$.

Standard deviations $\sigma_{\hat{\chi}_i}$ can be estimated assuming that $\mathbf{W}$ is a deterministic matrix and ρ is a zero mean additive independent noise [27] with a covariance matrix $\mathbf{C}_{\rho\rho}$, such that

$$\mathbf{C}_{\rho\rho} = E\left[\rho\rho^T\right] = \sigma^2_\rho \mathbf{I}_{r_c} \tag{45}$$

E is the expectation operator, and $\mathbf{I}_{r_c}$ is the $(r_c \times r_c)$ identity matrix. An unbiased estimation of the standard deviation σ_ρ is

$$\sigma^2_\rho = \|\mathbf{Y} - \mathbf{W}\hat{\chi}\|^2/(r_c - n_b) \tag{46}$$

The covariance matrix of the estimation error is given by

$$\mathbf{C}_{\hat{\chi}\hat{\chi}} = E\left[(\chi - \hat{\chi})(\chi - \hat{\chi})^T\right] = \sigma^2_\rho(\mathbf{W}^T\mathbf{W})^{-1} \tag{47}$$

$\sigma^2_{\hat{\chi}_i} = \mathbf{C}_{\hat{\chi}\hat{\chi}}(i,i)$ is the ith diagonal coefficient of $\mathbf{C}_{\hat{\chi}\hat{\chi}}$ (47).

The ordinary LS can be improved by taking into account different standard deviations on actuated joint j equations errors [27]. Data in $\mathbf{Y}$ and $\mathbf{W}$ of Eq. (40) are weighted with the inverse of the standard deviation of the error calculated from ordinary LS solution of the equations of joint j [27]

$$\mathbf{Y}^j = \mathbf{W}^j \chi + \rho^j \tag{48}$$

This weighting operation normalizes the errors in Eq. (40) and gives the weighted LS estimation of the parameters (IDIM-WLS).

4.3 Payload Identification. In order to identify both the robot and the payload dynamic parameters, using the model (38), it is necessary that the robot carries out two types of trajectories [30]

(1) Trajectories without payload and
(2) trajectories with payload fixed to the end-effector.

The sampling and filtering of the model IDIM (38) can be then written as

$$\mathbf{Y} = \begin{bmatrix} \mathbf{W}_a & \mathbf{0} \\ \mathbf{W}_b & \mathbf{W}_l \end{bmatrix} \begin{bmatrix} \chi \\ \chi_l \end{bmatrix} + \rho \tag{49}$$

where $\mathbf{W}_a$ is the observation matrix of the robot in the unloaded case, $\mathbf{W}_b$ is the observation matrix of the robot in the loaded case, and $\mathbf{W}_l$ is the observation matrix of the robot corresponding to the payload inertial parameters.

Thus, these two types of trajectories avoid the regrouping of the payload parameters with those of the platform and allow their independent identification. Section 5 presents experimental results on a prototype of actuation-redundant parallel robot.

5 Case Study

5.1 Description of the DualV. The DualV (Fig. 3) is a prototype of a planar parallel robot with actuation redundancy developed at the LIRMM [21]. This robot has three-controlled DOF (two translations in the plane (xOy) and one rotation about the z axis), but four identical legs with one actuator per leg. Thus, its degree of redundancy is equal to one. Each leg is composed of one proximal and one distal link. The proximal link A_iB_i is attached to the base by an actuated revolute joint and to the distal link B_iC_i by a passive revolute joint. The distal link is also attached to the moving platform by a passive revolute joint.

The geometric parameters of the virtual open-loop tree structure are described in Table 1 using the modified Denavit and Hartenberg notation (MDH) [14] (in this table, $\gamma_1 = 15.52$ deg, $\gamma_2 = 164.48$ deg, $\gamma_3 = -164.48$ deg, and $\gamma_4 = -15.52$ deg). The platform and payload are considered as supplementary bodies, the payload being fixed on the platform. They are, respectively, numbered as bodies 4 and 5.

Table 1 MDH parameters for the frames corresponding to *i*th robot leg ($i = 1, ..., 4$)

ji	a_{ji}	μ_{ji}	γ_{ji}	d_{ji}	θ_{ji}	r_{ji}
$1i$	0	1	γ_i	$l_{OA_i} = 0.41$ m	$q_{1i} - \gamma_i$	0
$2i$	$1i$	0	0	$l_{A_iB_i} = 0.28$ m	q_{2i}	0
$3i$	$2i$	0	0	$l_{B_iC_i} = 0.28$ m	q_{3i}	0

The DualV is actuated by four ETEL RTMB0140-100 direct drive actuators, which can deliver maximal torques of 127 Nm. The robot is able to achieve accelerations of 25 G in its workspace. The current amplifier can provide directly the measure of the input torque produced by the actuator.

Its controller is an augmented proportional derivative (PD) control with a dynamic based feedforward and internal-stress avoidance described in Fig. 4. PD controller gains are computed based on the response of a second-order differential equation for the tracking error equations, with a chosen bandwidth whose cutoff frequency is equal to $f_c = 70$ Hz ($\omega_c = 2\pi f_c$) and a damping factor $\xi = 0.7$ to provide the fastest response. The bandwidth is chosen just below the natural frequency of the robot estimated at about 100 Hz using finite element analysis.

The derivative term is filtered using a first-order low-pass filter whose cutoff frequency is set to 70 Hz to avoid amplifying noise. On this controller, we can switch on or off feed-forward terms to partially compensate for the dynamics of the system or not. This compensation is based on the inverse dynamics computation.

To get rid of the combination of joint torques that create internal-stress rather than operational forces, a projection along the null space of the robot inverse transposed Jacobian matrix $\mathbf{J}_p^{\text{inv T}}$ is performed

$$\tau^* = \tau - \sum_{i=1}^{n-r} \left(\mathbf{u}_{2_i}^{c\mathrm{T}} \tau \right) \mathbf{u}_{2_i}^c \tag{50}$$

where $\mathbf{u}_{2_i}^c$ $(i = 1, \ldots, n-r)$ span the null space of $\mathbf{J}_p^{\text{inv T}}$ (see Ref. [20]). Canceling internal-stress (from a kinetostatic point of view) is recommended since it leads to less deformation and impact favorably robot's accuracy. Additionally, it ensures having the joint torque vector of the lowest norm, which is good from an energy consumption point of view.

Finally, it should be mentioned here that, for the DualV, the controller is known and the value of the overconstraint could be fixed to zero in the identification procedure. However, this could not be the case if the robot was designed by industrial manufacturers that generally give few details about their technology.

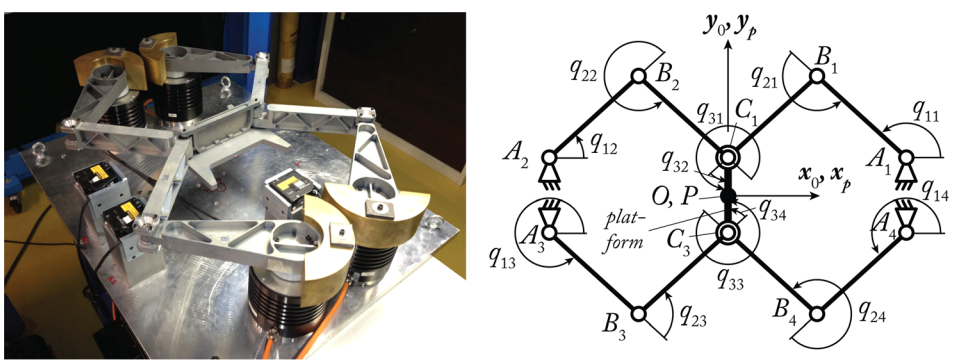

(a) (b)

Fig. 3 The DualV: (*a*) prototype of DualV robot and (*b*) kinematic description of DualV in a configuration where base frame x_0Oy_0 coincides with platform frame x_pPy_p

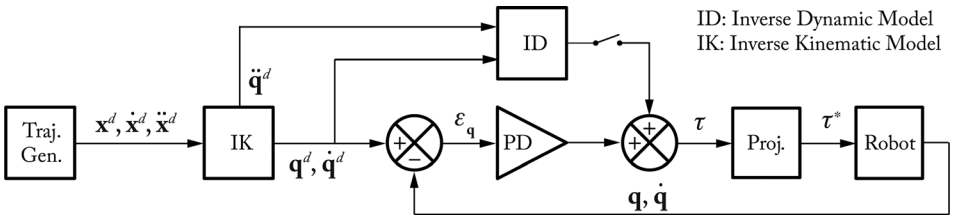

Fig. 4 The controller for the DualV

5.2 Computation of the Inverse Dynamic Model. The inverse dynamic model of the DualV can be obtained using the equations given in Secs. 2 and 3 but is detailed here for reason of clarity.

5.2.1 Inverse Dynamic Model of the Virtual Tree Structure and of the Virtual Free Platform. The inverse dynamic model of the open-loop virtual structure can be obtained by noticing that each leg is indeed a planar $3R$ robot in which the last body is massless. Its inverse dynamic model may be found in Ref. [31]

$$\begin{aligned}
\tau_{t_{1i}} = {} & \left(zz_{1i} + ia_{1i} + d_2^2 m_{2i}\right)\ddot{q}_{1i} + zz_{2i}(\ddot{q}_{1i} + \ddot{q}_{2i}) \\
& + d_2 mx_{2i}((2\ddot{q}_{1i} + \ddot{q}_{2i})\cos q_{2i} - \dot{q}_{2i}(2\dot{q}_{1i} + \dot{q}_{2i})\sin q_{2i}) \\
& + d_2 my_{2i}((2\ddot{q}_{1i} + \ddot{q}_{2i})\sin q_{2i} + \dot{q}_{2i}(2\dot{q}_{1i} + \dot{q}_{2i})\cos q_{2i}) \\
& + fs_{1i}\mathrm{sign}(\dot{q}_{1i}) + fv_{1i}\dot{q}_{1i} \\
\tau_{t_{2i}} = {} & zz_{2i}(\ddot{q}_{1i} + \ddot{q}_{2i}) + d_2 mx_{2i}\left(\ddot{q}_{1i}\cos q_{2i} + \dot{q}_{1i}^2 \sin q_{2i}\right) \\
& + d_2 my_{2i}\left(\ddot{q}_{1i}\sin q_{2i} - \dot{q}_{1i}^2 \cos q_{2i}\right) \\
& + fs_{2i}\mathrm{sign}(\dot{q}_{2i}) + fv_{2i}\dot{q}_{2i} \\
\tau_{t_{3i}} = {} & fs_{3i}\mathrm{sign}(\dot{q}_{3i}) + fv_{3i}\dot{q}_{3i}
\end{aligned} \tag{51}$$

where parameters zz_{ji}, ia_{ji}, m_{ji}, mx_{ji}, my_{ji}, fs_{ji}, and fv_{ji} are defined in Sec. 2.2 ($j = 1, 2, 3$), angles q_{ji} and length d_2 are defined in Table 1 and Fig. 3 ($j = 1, 2, 3$), $\tau_{t_{1i}}$ is the torque of the virtual actuator located at point A_i, $\tau_{t_{2i}}$ is the torque of the virtual actuator located at point B_i, and $\tau_{t_{3i}}$ is the torque of the virtual actuator located at point C_i. The vector $\tau_{\mathrm{idm_t}}$ of Eq. (1) stacks all vectors $\tau_{t_i} = [\tau_{t_{1i}} \tau_{t_{2i}} \tau_{t_{3i}}]^{\mathrm{T}}$.

The inverse dynamic model of the free body corresponding to the platform (body 4) with the payload (body 5) in the virtual system is

$$\begin{aligned}
\tau_{p_1} = {} & (m_4 + m_5)\ddot{x} - (mx_4 + mx_5)(\ddot{\phi}\sin\phi + \dot{\phi}^2\cos\phi) \\
& + (my_4 + my_5)(-\ddot{\phi}\cos\phi + \dot{\phi}^2\sin\phi) \\
\tau_{p_2} = {} & (m_4 + m_5)\ddot{y} + (mx_4 + mx_5)(\ddot{\phi}\cos\phi - \dot{\phi}^2\sin\phi) \\
& - (my_4 + my_5)(\ddot{\phi}\sin\phi + \dot{\phi}^2\cos\phi) \\
\tau_{p_3} = {} & (zz_4 + zz_5)\ddot{\phi} + (mx_4 + mx_5)(\ddot{y}\cos\phi - \ddot{x}\sin\phi) \\
& - (my_4 + my_5)(\ddot{y}\sin\phi + \ddot{x}\cos\phi)
\end{aligned} \tag{52}$$

with τ_{p_j} being the jth components of the vector τ_p of Eq. (6); x, y, and ϕ are the platform coordinates (x and y are the position of the platform center; ϕ is the platform orientation defined as the angle between the axes x_0 and x_p); and zz_j, m_j, mx_j, and my_j are defined in Sec. 2.2 ($j = 4, 5$).

From Eqs. (51) and (52), the identification model of the tree structure and of the free platform can easily be obtained.

The way to compute the platform and the virtual tree structure joint coordinates, velocities, and accelerations is detailed in the Sec. 5.2.2.

5.2.2 FKP of the Real Parallel Robot. For the DualV, the loop-closure equations (7) can be written as (for $i = 1\ldots4$)

$$\begin{aligned}
0 &= x - r_{\mathrm{p}}\sin(\phi + k\pi) - x_{A_i} - d_2\cos q_{1i} - d_3\cos(q_{1i} + q_{2i}) \\
0 &= y + r_{\mathrm{p}}\cos(\phi + k\pi) - y_{A_i} - d_2\sin q_{1i} - d_3\sin(q_{1i} + q_{2i}) \\
0 &= \phi + \bar{k}\pi - q_{1i} - q_{2i} - q_{3i}
\end{aligned} \tag{53}$$

where r_{p} is the half platform length ($r_{\mathrm{p}} = l_{C_1C_3}/2$), $k = 0$ ($\bar{k} = 1$) if $i = 1, 2$, $k = 1$ ($\bar{k} = 0$) if $i = 3, 4$, and x_{A_i} and y_{A_i} are the position coordinates along $\mathbf{x}$ and $\mathbf{y}$ axes for the point A_i.

From the two first lines of Eq. (53), the reduced loop-closure equation (8) that directly relate the displacements of the actuated joints to the moving platform coordinates can be obtained after deleting from these expressions the terms in $\cos q_{2i}$ or $\sin q_{2i}$ (for $i = 1\ldots4$)

$$d_3^2 = (x_{C_i} - x_{B_i})^2 + (y_{C_i} - y_{B_i})^2 \tag{54}$$

where $x_{C_i} = x - r_{\mathrm{p}}\sin(\phi + k\pi)$ and $y_{C_i} = y + r_{\mathrm{p}}\cos(\phi + k\pi)$ are the position coordinates of point C_i, and $x_{B_i} = x_{A_i} + d_2\cos q_{1i}$ and $y_{B_i} = y_{A_i} + d_2\sin q_{1i}$ are the position coordinates of point B_i.

Noticing that the forward geometric problem can be solved by

$$x = \frac{x_{C_1} + x_{C_3}}{2}, \quad y = \frac{y_{C_1} + y_{C_3}}{2}, \quad \phi = \tan^{-1}\left(-\frac{x_{C_1} - x_{C_3}}{y_{C_1} - y_{C_3}}\right) \tag{55}$$

when finding expressions of x_{C_j} and y_{C_j} ($j = 1, 3$) as functions of q_{1i} ($i = 1\ldots4$). These expressions are quite simple to find as the loops formed by the legs 1 and 2, or the legs 3 and 4, are five-bar linkages

$$x_{C_j} = f_j y_{C_j} + k_j, y_{C_j} = \frac{-p_j \pm \sqrt{p_j^2 - 4g_j r_j}}{2g_j} \tag{56}$$

where

$$\begin{aligned}
f_j &= -\frac{y_{B_{j+1}} - y_{B_j}}{x_{B_{j+1}} - x_{B_j}}, \quad g_j = f_j^2 + 1 \\
k_j &= \frac{x_{B_j}^2 + y_{B_j}^2 - y_{B_j}^2 - y_{B_{j+1}}^2}{2(x_{B_{j+1}} - x_{B_j})} \\
p_j &= 2f_j(k_j - x_{B_j}) - 2y_{B_j} \\
r_j &= x_{B_j}^2 + y_{B_j}^2 - d_3^2 + k_j^2 - 2k_j x_{B_j}
\end{aligned} \tag{57}$$

In Eq. (56), the sign "$\pm$" denotes the two robot assembly modes that are considered to be a priori fixed in the identification process as no parallel singularities are crossed.

Then, it comes easily from Eq. (53) that

$$q_{2i} = \tan^{-1}\left(\frac{y_{C_i} - y_{B_i}}{x_{C_i} - x_{B_i}}\right) - q_{1i}, \quad q_{3i} = \phi + \bar{k}\pi - q_{1i} - q_{2i} \tag{58}$$

Table 2 Essential parameters of the DualV

Param.	Case 1 Id. Val.	$\%\sigma_{\hat{\chi}_i}$	Case 2 Id. Val.	$\%\sigma_{\hat{\chi}_i}$
zz_{11R}	4.45×10^{-2}	1.58	4.12×10^{-2}	3.14
zz_{12R}	4.81×10^{-2}	1.39	4.62×10^{-2}	3.09
zz_{13R}	4.81×10^{-2}	1.41	4.57×10^{-2}	2.54
zz_{14R}	5.07×10^{-2}	1.38	5.79×10^{-2}	1.89
zz_4	2.06×10^{-2}	1.37	2.05×10^{-2}	2.23
m_4	1.92×10^{0}	1.08	1.96×10^{0}	1.48
zz_5	1.61×10^{-2}	1.71	1.64×10^{-2}	3.04
mx_5	-1.27×10^{-1}	0.76	-1.27×10^{-1}	1.51
m_5	5.42×10^{0}	0.30	5.52×10^{0}	0.29

Relative error norm $\|\rho\|/\|\mathbf{Y}\| \Rightarrow$ Case 1: 0.110 and Case 2: 0.091.

Then, differentiating Eqs. (53) and (54) with respect to time, and simplifying, the matrices $\mathbf{A}_p, \mathbf{B}_p, \mathbf{J}_k$ and $\mathbf{J}_{\text{tk}}$ of Eq. (13) can be found

$$\mathbf{a}_p^i = d_3[\,c_{12i} \quad s_{12i} \quad -\sin(\phi+k\pi)s_{12i}+\cos(\phi+k\pi)c_{12i}\,] \tag{59}$$

where $\mathbf{a}_p^i$ is the ith line of $\mathbf{A}_p$, $c_{12i}=\cos(q_{1i}+q_{2i})$ and $s_{12i}=\sin(q_{1i}+q_{2i})$

$$b_p^{ii} = d_2 d_3 \sin q_{2i} \tag{60}$$

where b_p^{ii} is the ith term of the diagonal matrix $\mathbf{B}_p$

$$\mathbf{J}_{\text{tk}}^{\text{T}} = \left[\,\mathbf{J}_{\text{tk}}^{1\text{T}} \quad \mathbf{J}_{\text{tk}}^{2\text{T}} \quad \mathbf{J}_{\text{tk}}^{3\text{T}} \quad \mathbf{J}_{\text{tk}}^{4\text{T}}\,\right] \tag{61}$$

in which, for $i=1\ldots4$

$$\mathbf{J}_{\text{tk}}^i = \begin{bmatrix} 1 & 0 & -r_{\text{p}}\cos(\phi+k\pi) \\ 0 & 1 & -r_{\text{p}}\sin(\phi+k\pi) \\ 0 & 0 & 1 \end{bmatrix} \tag{62}$$

and $\mathbf{J}_k$ is a block-diagonal matrix whose ith diagonal element is

$$\mathbf{J}_k^i = \begin{bmatrix} -d_2\sin q_{1i} - d_3\sin(q_{1i}+q_{2i}) & -d_3\sin(q_{1i}+q_{2i}) & 0 \\ d_2\cos q_{1i} + d_3\cos(q_{1i}+q_{2i}) & d_3\cos(q_{1i}+q_{2i}) & 0 \\ 1 & 1 & 1 \end{bmatrix} \tag{63}$$

Then, all velocities can be computed from Eqs. (9) and (21) as a function $\dot{\mathbf{q}}^{\text{T}} = [\dot{q}_{11}\ \dot{q}_{12}\ \dot{q}_{13}\ \dot{q}_{14}]^{\text{T}}$

$$\mathbf{t} = \begin{bmatrix} \dot{x} \\ \dot{y} \\ \dot{\phi} \end{bmatrix} = -\mathbf{A}_p^{+}\mathbf{B}_p\dot{\mathbf{q}}, \dot{\mathbf{q}}_i = \left(\mathbf{J}_k^i\right)^{-1}\mathbf{J}_{\text{tk}}^i\mathbf{t} \tag{64}$$

where $\dot{\mathbf{q}}_i$ is the vector of the leg i joint velocities.

Finally, the accelerations can be computed from Eqs. (10) and (24) using the previous expressions. Combining these expressions with those of Sec. 5.2.2 into the equations of Sec. 3, the identification models of the DualV can be computed.

5.3 Identification Results. In this part, experimentations are performed and the dynamic identification model is carried out on the DualV using the modeling approaches presented in Sec. 3 and the identification procedure proposed in Sec. 4. To estimate the quality of the identification procedure, a payload mass of 5.37 kg which has been accurately weighed is mounted of the platform and will be identified in parallel to the robot parameters. Two types of exciting trajectories are then performed, as explained in Sec. 4.3

(1) Trajectories without the payload
(2) Trajectories with the payload fixed to the end-effector

Before presenting the identification result, it should be noticed that during identification process, some small base parameters remain poorly identifiable because they have no significant contribution in the joint torques. They are canceled to keep a set of

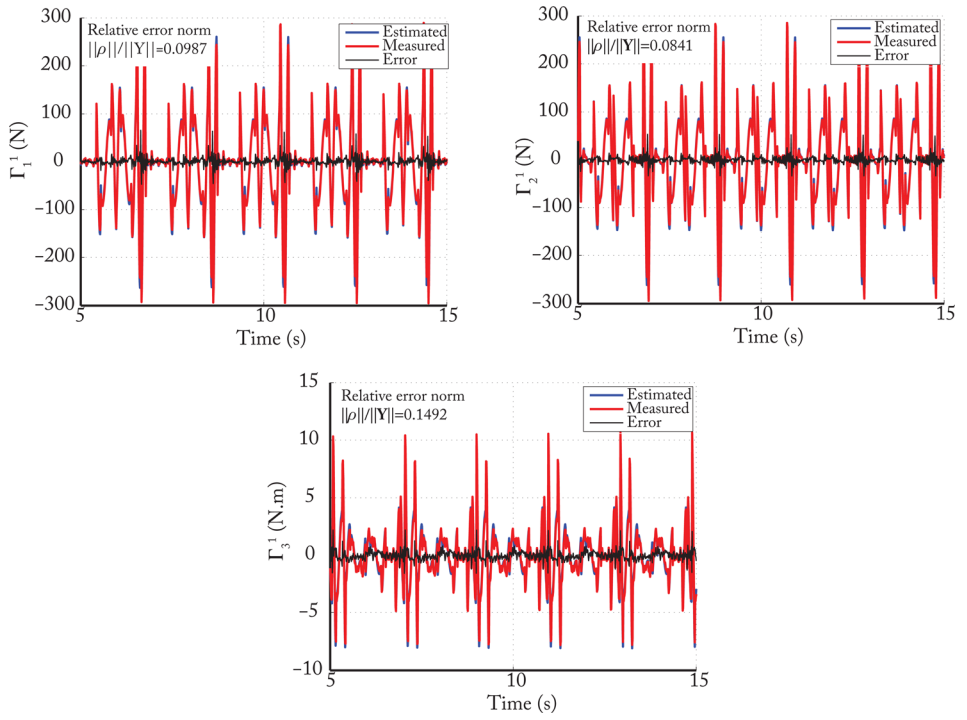

Fig. 5 Values of Γ^1, estimated from input torques using the relation $\mathbf{J}_\rho^{\text{inv}T}\tau$ from Eq. (30) (red lines) and calculated using identified parameters $\hat{\chi}$ from the relation $\text{IDM}\chi$ (blue lines) with the payload of 5.37 kg

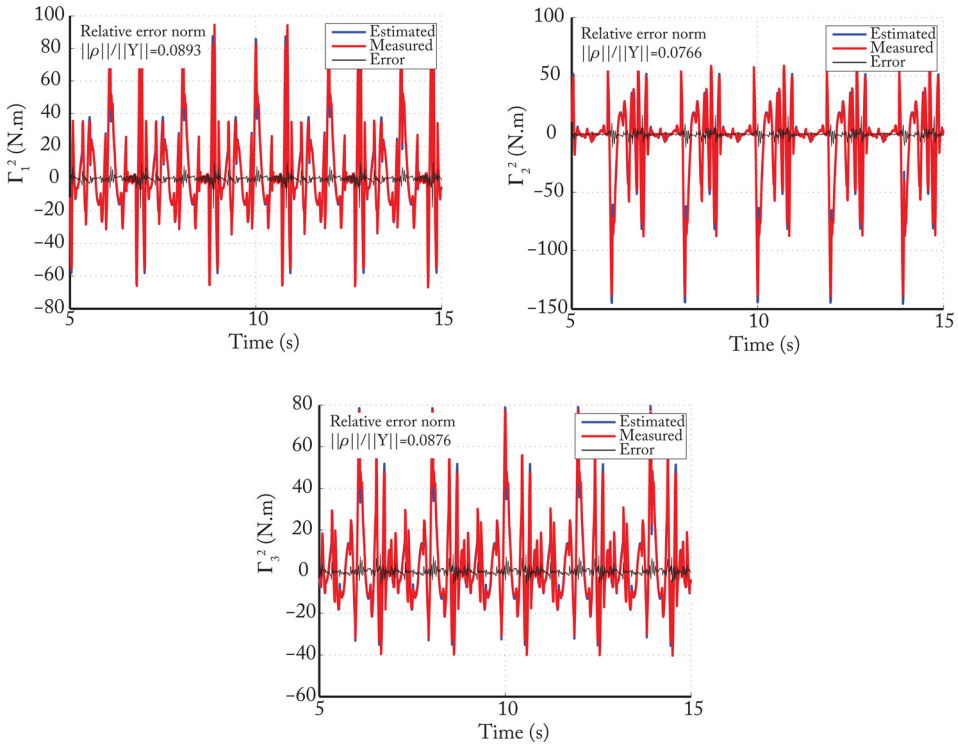

Fig. 6 Values of Γ^2, estimated from input torques using the relation $\tau^{1:3} - \mathbf{J}_{\tau_4}^T \tau^4$ from Eq. (36) (red lines) and calculated using identified parameters $\hat{\chi}$ from the relation $\mathbf{IDM}\chi$ (blue lines) with the payload of 5.37 kg

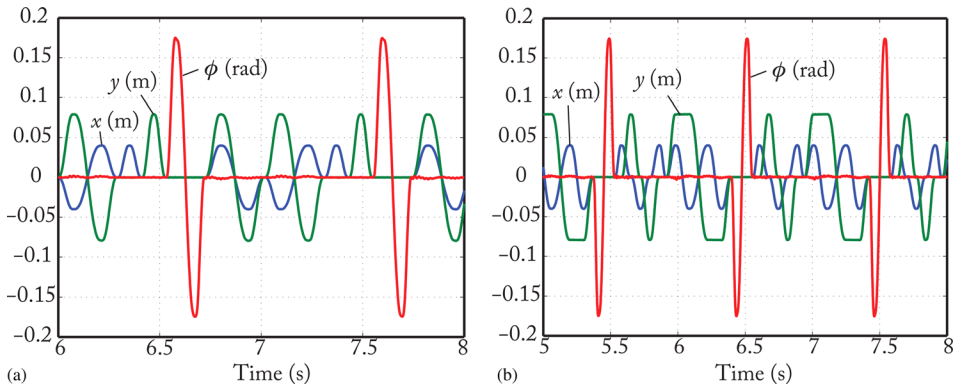

Fig. 7 The two trajectories used for the cross-validations: (*a*) trajectory 1 and (*b*) trajectory 2

essential parameters of a simplified dynamic model with a good accuracy [9]. The essential parameters are calculated using an iterative procedure starting from the base parameters estimation. At each step, the base parameter which has the largest relative standard deviation $\%\sigma_{\hat{\chi}_{ri}}$ is canceled. A new IDIM-WLS parameter estimation of the simplified model is carried out with new relative error standard deviations $\%\sigma_{\hat{\chi}_{ri}}$. The procedure ends when $\max(\%\sigma_{\hat{\chi}_{ri}})/\min(\%\sigma_{\hat{\chi}_{ri}}) < r_\sigma$, where r_σ is a ratio ideally chosen between 10 and 30 depending on the level of perturbation in $\mathbf{Y}$ and $\mathbf{W}$. In the following of the paper, this ratio is fixed to ten.

The two proposed identification models are tested:

Case 1 The IDIM of Sec. 3.1.1 projects the input torques on the platform and

Case 2 The IDIM of Sec. 3.1.2 for which the input torque 4 is projected on the actuators 1–3.

Table 3 Relative error norms (percent)

	Trajectory 1				Trajectory 2				
$\hat{\chi}$	τ_1	τ_2	τ_3	τ_4	τ_1	τ_2	τ_3	τ_4	Mean
Case 1	9.1	8.5	7.5	8.9	9.8	8.5	7.6	10.5	8.8
Case 2	9.1	8.5	8.0	8.6	10.0	8.6	8.2	11.7	9.2

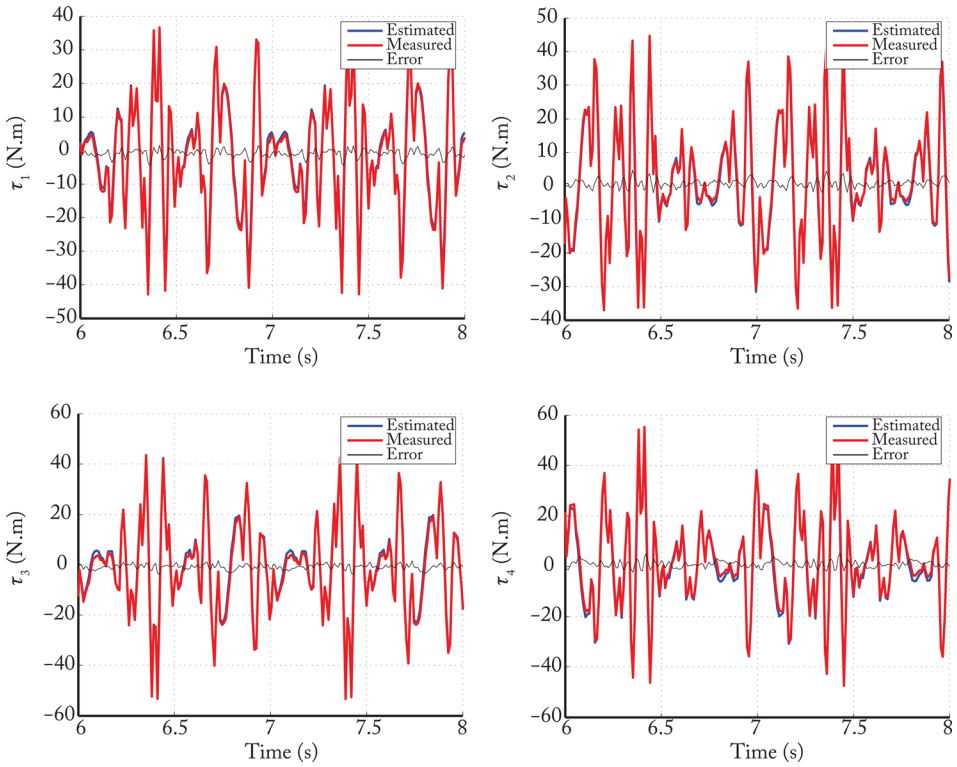

Fig. 8 Measured (red lines) and estimated (blue lines) input torques rebuilt using the identified parameters of case 1 on trajectory 1

Table 2 presents the identification results. Subscript R stands for the parameters that have been regrouped using the procedure presented in Sec. 4.1 (here, $zz_{1i_R} = zz_{1i} + ia_{1i} + d_2^2 m_{2i}$). It can be observed that the robot parameters have been correctly estimated in both cases. The payload of 5.37 kg has also been accurately identified. Moreover, the relative error norms in both cases are about 10%, which shows that the inputs Γ^j have been correctly reconstructed (see also Figs. 5 and 6).

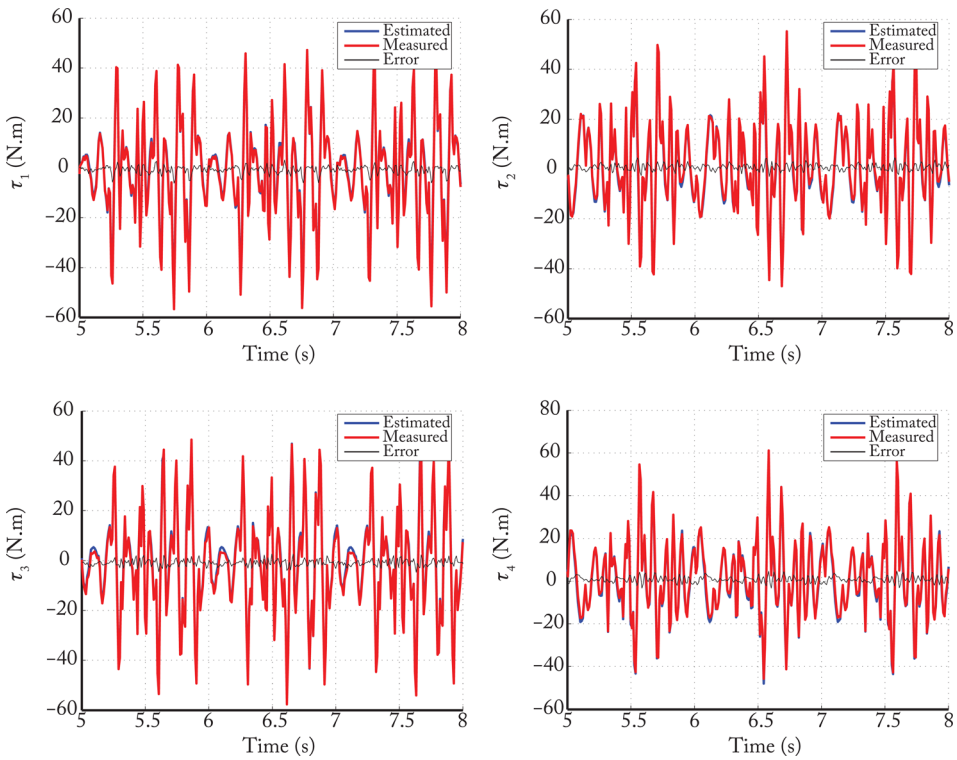

Fig. 9 Measured (red lines) and estimated (blue lines) input torques rebuilt using the identified parameters of case 1 on trajectory 2

Table 4 Tracking errors (10^{-3} rad)

	Trajectory 1				Trajectory 2			
	e_1	e_2	e_3	e_4	e_1	e_2	e_3	e_4
Case a	6.35	6.50	8.00	8.25	7.70	7.65	9.40	7.60
Case b	2.79	2.15	1.95	2.10	2.90	2.65	2.20	2.05
Case c	2.80	2.11	2.06	2.04	2.83	2.67	2.25	2.10
b/a (%)	55.9	66.9	75.6	74.6	62.3	65.4	76.6	73.0
c/a (%)	56.0	67.6	74.3	75.2	63.2	65.1	76.1	72.3

Note: $e_i = \max\left|q_i^{\mathrm{d}} - q_i^{\mathrm{m}}\right|$, where q_i^{d} and q_i^{m} are the desired and measured joint i positions, respectively. b/a (c/a) (%): percentage of error reduction between cases a and b (c).

However, the IDIM of case 1 leads to lower standard deviations of the identified parameters and to the best payload estimation.

5.4 Cross-Validations. To cross-validate the obtained models, the following procedure is used. First, a computed torque control scheme is implemented into the controller. This scheme uses the dynamic models identified into the previous part. Into the controller, the value of the overcontraint is set to zero (Eq. (26)).

Then, two different trajectories are performed and input torques measurements are recorded during these movements. The two trajectories are depicted in Fig. 7. It should be mentioned that, obviously, they are different from the trajectory used for the identification process.

Finally, the measured torques are compared with the calculated torques using Eq. (26) by setting the value of the overcontraint equal to zero. The results, in terms of relative error norms, are summarized in Table 3 (see also Figs. 8 and 9 that show the torques along the two trajectories with the parameters identified in case 1). It can be seen that the input torques are correctly predicted in both cases, even if the parameters identified with the IDIM of case 1 lead to a slightly better torque estimation.

Finally, to see the improvement in terms of trajectory tracking, the tracking errors obtained when:

Case a: A simple PD control scheme is implemented into the controller,

Case b: A computed torque control scheme is implemented into the controller (with parameters identified in case 1), and

Case c: A computed torque control scheme is implemented into the controller (with parameters identified in case 2).

The maximal tracking errors for each joint are given in Table 4. Of course, when computed torque control is used, the tracking error is lower (from 54% to 76% of reduction). The comparison between the cases b and c, when computed torque control is used with the two different identified dynamic parameters, is more difficult to carry out. Indeed, both controllers are quite equivalent in terms of tracking errors. Therefore, it is not possible to claim which kind of identification methodology is better.

5.5 Discussion. It has been observed for the DualV that, even if the results are slightly the same in terms of tracking errors, the IDIM model of Sec. 3.1.1 leads to better parameter estimation and torque reconstruction. However, these results are not sufficient for stating that, in general, the best IDIM to use is the one of Sec. 3.1.1. This should be confirmed after carrying out many experiments on different types of actuation-redundant robots, and even if we had the possibility to do so, this is not the topic of the present paper. Moreover, even if for the moment we have no example in mind, we think that it could exist some particular robots for which the IDIM of Sec. 3.1.2 is better suited.

To our opinion, the only thing it is possible to claim is that the computation of the IDIM of Sec. 3.1.1 is more straightforward than the computation of the IDIM of Sec. 3.1.2 as all the equations are projected on the platform and as it cannot exist several combinations for projecting the equations.

6 Conclusion

This paper has presented a method for the identification of the inertial parameters of parallel robots with actuation redundancy. Contrary to serial robots or parallel robots without actuation redundancy for which the dynamic identification methods are based on the use of the IDIM which calculates each joint force/torque that is linear in relation to the dynamic parameters, for actuation-redundant parallel robots that are overconstrained, the usual IDIM has an infinity of solutions for the force/torque prediction, depending of the value of the desired overconstraint that is a priori unknown. As a result, the usual IDIM cannot be used as it is.

This paper proposed a universal procedure for the computation of a modified IDIM of actuation-redundant parallel robots, i.e., which can be applied for any actuation-redundant parallel robot *for which the value of the overconstraint is known or not*. Two modified formulations have been shown for the IDIM of actuation-redundant robots that can be used for identification purpose. This formulation consists of projecting the input torques/forces on other bodies, thus leading to unique solution of the model that can thus be used in the identification process. The identification of the inertial parameters of a planar parallel robot with actuation redundancy, the DualV, was then performed using these modified IDIM. Experimental results show that the inertial parameters of the robot were correctly identified. Moreover, for validation purpose, a known payload mass has been added on the robot to be sure that the identification process was correct. This mass has been very accurately identified. Finally, it has been shown that the torque prediction with the newly identified parameters was correct and that when the identified models were used into controller with torque prediction, the tracking errors were considerably lower.

Acknowledgment

This work has been partially funded by the French ANR Project ARROW (No. ANR 2011 BS3 006 01).

References

[1] Merlet, J., 2006, *Parallel Robots*, 2nd ed., Springer, New York.
[2] Yi, B., Freeman, R., and Tesar, D., 1994, "Force and Stiffness Transmission in Redundantly Actuated Mechanisms: The Case for a Spherical Shoulder Mechanism," Rob., Spat. Mech., Mech. Syst., **45**, pp. 163–172.
[3] Kurtz, R., and Hayward, V., 1992, "Multiple-Goal Kinematic Optimization of a Parallel Spherical Mechanism With Actuator Redundancy," IEEE Trans. Rob. Autom., **8**(5), pp. 644–651.
[4] Nahon, M. A., and Angeles, J., 1989, "Force Optimization in Redundantly-Actuated Closed Kinematic Chains," International Conference on Robotics and Automation, Scottsdale, AZ, May 14–19, pp. 951–956.
[5] Muller, A., 2005, "Internal Preload Control of Redundantly Actuated Parallel Manipulators—Its Application to Backlash Avoiding Control," IEEE Trans. Rob., **21**(4), pp. 668–677.
[6] Cheng, H., Yiu, Y.-K., and Li, Z., 2003, "Dynamics and Control of Redundantly Actuated Parallel Manipulators," IEEE/ASME Trans. Mechatronics, **8**(4), pp. 483–491.
[7] Hanon, M. A., 1995, "Comparison of Methods for the Control of Redundantly-Actuated Robotic Systems," J. Intell. Rob. Syst., **14**, pp. 3–21.

[8] Muller, A., 2005, "Internal Prestress Control of Redundantly Actuated Parallel Manipulators Its Application to Backlash Avoiding Control," IEEE Trans. Rob., **21**(4), pp. 668–677.
[9] Khalil, W., Gautier, M., and Lemoine, P., 2007, "Identification of the Payload Inertial Parameters of Industrial Manipulators," IEEE ICRA, Rome, Italy, Apr. 10–14, pp. 4943–4948.
[10] de Wit, C. C., and Aubin, A., 1990, "Parameters Identification of Robots Manipulators Via Sequential Hybrid Estimation Algorithms," IFAC Congress, pp.178–183.
[11] Antonelli, G., Caccavale, F., and Chiacchio, P., 1999, "A Systematic Procedure for the Identification of Dynamic Parameters of Robot Manipulators," Robotica, **17**(4), pp. 427–435.
[12] Kozlowski, K., 1998, *Modelling and Identification in Robotics*, Springer, London.
[13] Hollerbach, J., Khalil, W., and Gautier, M., 2008, *Handbook of Robotics—Model Identification*, Springer, New York.
[14] Khalil, W., and Dombre, E., 2002, *Modeling, Identification and Control of Robots*, Hermes Penton, London.
[15] Khosla, P., and Kanade, T., 1988, "Parameter Identification of Robot Dynamics," 24th IEEE CDC, pp. 1754–1760.
[16] Lu, Z., Shimoga, K., and Goldenberg, A., 1993, "Direct Calculation of Minimum Set of Inertial Parameters of Serial Robots," J. Rob. Syst., **10**(8), pp. 1009–1029.
[17] Restrepo, P., and Gautier, M., 1995, "Calibration of Drive Chain of Robot Joints," Fourth IEEE Conference on Control Applications, Albany, NY, Sept. 28–29, pp. 526–531.
[18] Corke, P., 1996, "In Situ Measurement of Robot Motor Electrical Constants," Robotica, **23**(14), pp. 433–436.
[19] Gautier, M., and Briot, S., 2014, "Global Identification of Joint Drive Gains and Dynamic Parameters of Robots," ASME J. Dyn. Sys. Meas. Control, **136**(5), p. 051025.
[20] Hufnagel, T., and Müller, A., 2012, "A Projection Method for the Elimination of Contradicting Decentralized Control Forces in Redundantly Actuated PKM," IEEE Trans. Rob., **28**(3), pp. 723–728.
[21] van der Wijk, V., Krut, S., Pierrot, F., and Herder, J., 2011, "Generic Method for Deriving the General Shaking Force Balance Conditions of Parallel Manipulators With Application to a Redundant Planar 4-RRR Parallel Manipulator," 13th World Congress in Mechanism and Machine Science, pp. 1822–1827.
[22] Briot, S., Gautier, M., and Krut, S., 2013, "Dynamic Parameter Identification of Actuation Redundant Parallel Robots: Application to the DualV," IEEE/RSJ International Conference on Intelligent Robots and Systems, Wollongong, NSW, July 9–12, pp. 637–643.
[23] Briot, S., and Gautier, M., 2012, "Global Identification of Drive Gains and Dynamic Parameters of Parallel Robots—Part 1: Theory," 19th CISM-IFToMM Symposium on Robot Design, Dynamics, and Control (RoManSy), pp. 93–100.
[24] Pfurner, M., and Husty, M., 2010, "Implementation of a New and Efficient Algorithm for the Inverse Kinematics of Serial 6R Chains," *New Trends in Mechanism Science*, Springer, New York, pp. 91–98.
[25] Briot, S., and Arakelian, V., 2008, "Optimal Force Generation of Parallel Manipulators for Passing Through the Singular Positions," Int. J. Rob. Res., **27**(8), pp. 967–983.
[26] Nenchev, D. N., Bhattacharya, S., and Uchiyama, M., 1997, "Dynamic Analysis of Parallel Manipulators Under the Singularity-Consistent Parameterization," Robotica, **15**(4), pp. 375–384.
[27] Gautier, M., 1997, "Dynamic Identification of Robots With Power Model," IEEE ICRA, Albuquerque, NM, Apr. 20–25, pp. 1922–1927.
[28] Gautier, M., 1991, "Numerical Calculation of the Base Inertial Parameters," J. Rob. Syst., **8**(4), pp. 485–506.
[29] Diaz-Rodriguez, M., Mata, V., Valera, A., and Page, A., 2010, "A Methodology for Dynamic Parameters Identification of 3-D of Parallel Robots in Terms of Relevant Parameters," Mech. Mach. Theory, **45**(9), pp. 1337–1356.
[30] Khalil, W., and Ibrahim, O., 2007, "General Solution for the Dynamic Modeling of Parallel Robots," J. Intell. Rob. Syst., **49**(1), pp. 19–37.
[31] Gautier, M., Vandanjon, P., and Presse, C., 1994, "Identification of Inertial and Drive Gain Parameters of Robots," IEEE CDC, Lake Buena Vista, FL, Dec. 14–16, pp. 3764–3769.